Acta Neuropathol (1994) 87:554–567

REGULAR PAPER

Eva Braak · Heiko Braak · Eva-Maria Mandelkow

A sequence of cytoskeleton changes related to the formation of neurofibrillary tangles and neuropil threads

Received: 17 November 1993 / Revised, accepted: 10 January 1994

Abstract Frontal sections of the temporal lobe including the transentorhinal/entorhinal region, amygdala, and/or hippocampus from human adult brains are studied for cytoskeleton changes using immunostaining with the antibodies AT8 and Alz-50 and selective silver impregnation methods for neurofibrillary changes of the Alzheimer type. For the purpose of correlation, the two methods are carried out one after the other on the same section. Layer pre-α in the transentorhinal/entorhinal region harbours nerve cells which are among the first nerve cells in the entire brain to show the development of neurofibrillary changes. This presents the opportunity for study of both early events in the destruction of the cytoskeleton in individual neurons, and to relate changes which occur in the neuronal processes in the absence of alterations in their immediate surroundings to those happening in the soma. Immunoreactions with the AT8 antibody in particular reveal a clear sequence of changes in the neuronal cytoskeleton. Group 1 neurons present initial cytoskeleton changes in that the soma, dendrites, and axon are completely marked by granular AT8 immunoreactive material. These neurons appear quite normal and turn out to be devoid of argyrophilic material when observed in silver-stained sections. Group 2 neurons show changes in the cellular processes. The terminal tuft of the apical dendrite is replaced by tortuous varicose fibres and coarse granules. The distal protions of the dendrites are curved and show appendages and thickened portions. Intensely homogeneously immunostained rod-like inclusions are encountered in these thickened portions and in the soma. A number of these rod-like inclusions are visible after silver staining, as well. Group 3 neurons display even more pronounced alterations of their distal – most dendritic portions. The intermediate dendritic parts lose immunoreactivity, but the soma is homogeneously immunostained. Silver staining reveals in most of the distal dendritic parts neuropil threads, and in the soma a classic neurofibrillary tangle. Group 4 structures are marked by accumulations of coarse AT8-immunoreactive granules. Silver staining provides evidence that the fibrillary material has become an extraneuronal, "early" ghost tangle. Finally, group 5 structures present "late" ghost tangles in silver-stained sections but fail to demonstrate AT8 immunoreactivity. It is suggested that the altered tau protein shown by the antibody AT8 represents an early cytoskeleton change which eventually leads to the formation of argyrophilic neurofibrillary tangles and neuropil threads.

Key words Cytoskeleton · Neurofibrillary tangle Neuropil thread · Tau protein · Abnormal phosphorylation

Supported by the Deutsche Forschungsgemeinschaft

E. Braak (✉) · H. Braak
Zentrum der Morphologie, J.W. Goethe-Universität, Theodor Stern Kai 7, D-60590 Frankfurt/Main, Germany

E.-M. Mandelkow
Max Planck Gesellschaft, Arbeitsgruppe für strukturelle Molekularbiologie, DESY, Notkestrasse 85, D-22607 Hamburg, Germany

Introduction

Neurofibrillary tangles (NFT) and neuropil threads (NT [14]) are important morphological hallmarks of Alzheimer's disease (AD). Only a few types of nerve cells in the human brain are prone to develop NFT and NT. These pathological changes are first seen in a few limbic cortical areas, and from here the destructive process spreads in a predictable, non-random manner across the cortex and brain stem [11].

Abnormally phosphorylated microtubule-associated tau proteins are components of the fibrous material forming NFT and NT [21, 30, 34, 35, 43, 62]. They are located in paired helical filaments (PHF) and straight filaments [6, 20, 42, 48, 60]. The AT8 antibody is very sensitive in detecting abnormal phosphorylation of the tau protein without showing cross-reactivity with nor-

mal tau epitopes. AT8 recognises a phosphatase-sensitive epitope, the phosphorylated serines 199 and 202 in PHF-tau [4, 46, 55]. This antibody is particularly well suited to study the gradual development of NFT and NT.

By comparison, the known antibody Alz-50 [61] recognises an epitope near the amino terminus of the tau molecule independently of phosphorylation [17, 32, 33, 49, 56] and shows some cross-reactivity with normal tau protein [31, 44]. Therefore, it may be that Alz-50-immunoreactive structures are not seen exclusively in degenerative diseases [51].

Sections treated with sensitive silver techniques first display NFT and NT in the transentorhinal region. Initially, the changes are confined to the transentorhinal layer pre-α [9, 11]. Only the projection cells of this layer are capable of developing NFT and NT. Even mid-aged individuals frequently show the presence of a few transentorhinal NFT and NT. Brain tissue almost devoid of neurofibrillary changes or with only mild alterations is intentionally used in this study. Most of these cases are barren of extracellular amyloid deposits (diffuse plaques) and neuritic plaques. This offers the unique opportunity to study early events in the deterioration of the cytoskeleton in individual pyramidal cells in the absence of pathological changes in the surrounding tissue.

Nomenclature

In the human brain, the allocortical entorhinal region spreads over the ambient gyrus and the anterior parts of the parahippocampal gyrus. Laterally it is bordered by the transentorhinal region which mediates towards the temporal proisocortex. The entorhinal region displays a lamination pattern different from that of the isocortex. The uppermost cellular layer pre-α consists of islands of large multipolar neurons, the majority of which are considered to be modified pyramidal neurons, and the axons of which generate the perforant path. Within the transentorhinal region the pre-α islands amalgamate to form a plate which gradually sinks into a deeper position. On their way into this deeper position, the multipolar pre-α projection neurons become regularly aligned and are transformed into pyramidal neurons [9, 12, 13, 27].

The neuritic plaque comprises an accumulation of argyrophilic dystrophic neurites sometimes surrounding an amyloid core. A diffuse plaque represents a pure amyloid deposit which may vary in shape and size and is devoid of argyrophilic neurites.

Materials and methods

Brains from 32 individuals of both sexes (aged from 20 to 89 years), with no known neurological disease, were obtained at autopsy (Table 1). They were either fixed routinely by immersion in a aqueous solution of formaldehyde or for immunocytochemical investigations, by immersion in a mixture of 4 % paraformaldehyde and picric acid (pH 7; for details see [8]). Blocks of the temporal lobe including the entorhinal and transentorhinal regions, amygdala and/or hippocampal region were selected. Series of frontal sections (60–80 μm thick) were cut on a freezing microtome or a cryostat. The first and the last sections of each series were stained with aldehyde fuchsin/Darrow red for orientation [15]. Two sections were treated with selective silver stainings for demonstration of neurofibrillary changes [29] and of brain amyloid deposits [19]. The remaining sections were used for immunocytochemistry.

All cases were classified according to a stageing procedure, which permits differentiation between six stages with increasing severity of cortical neurofibrillary changes (Table 1; I-II: transentorhinal stages, III-IV: limbic stages, V-VI: isocortical stages = fully developed AD) and three stages of amyloid depositing (A: a few diffuse plaques in basal isocortex, B: many diffuse plaques in basal isocortex and allocortex, C: large numbers of diffuse plaques in all parts of the cortex [11, 16]).

Table 1 Data regarding the tissue examined. The stageing for neurofibrillary changes and for amyloid deposits is carried out according to [11]. Cases 24, 27, 30, 32 additionally exhibit argyrophilic grains [10] (*f* female, *m* male, *Neurofibr* neurofibrillary)

Case	Age (years)	Gender	Neurofibr. change stage	Amyloid deposits stage
01	20	m	0	0
02	26	m	0	0
03	32	f	0	0
04	40	m	0	0
05	41	m	I	A
06	44	m	0	0
07	44	f	II	0
08	47	m	0	0
09	51	f	I	0
10	51	m	0	0
11	55	f	II	0
12	57	m	I	0
13	61	f	I	A
14	61	f	I	B
15	64	m	II	0
16	64	f	0	0
17	66	m	III	B
18	68	m	I	0
19	68	f	I	0
20	69	m	0	B
21	70	m	I	B
22	71	f	I	0
23	73	m	III	B
24	75	m	I	A
25	77	m	II	0
26	77	f	II	0
27	78	f	II	0
28	79	f	III	A
29	81	m	I	B
30	85	f	I	B
31	87	f	II	A
32	89	f	I	B

Incubation of free floating sections was done with the following primary antibodies for about 40–44 h at 4°C: monoclonal AT8 (1:1000, [46]), and monoclonal Alz-50 (1:25, [61]). Incubation with the second biotinylated antibodies was performed for 2 h: anti-mouse IgG or anti-mouse IgM. Immunoreactions were visualised with the avidin-biotin-peroxidase complex (Vectastain) and 3-3-diaminobenzidine-4 HCl/H_2O_2 (DAB, D5637 Sigma) or with 4-chloro-1-naphthol/H_2O_2 (CN, C8890 Sigma). In addition, several sections were predigested with alkaline phosphatase prior to immunostaining with AT8.

Individual AT8- and Alz-50-immunostained sections of each series were used to compare directly the immunoreaction with the result of selective silver staining. In some AT8- and Alz-50-immunostained sections treated with CN, the immunoreactive neurons were photographed, in part with Nomarski contrast, and their exact positions were mapped by a vernier scale. The chromogen was destained with 70 % and 96 % ethanol for about 8–10 h.

The sections were restained by the Gallyas silver impregnation method for neurofibrillary changes [29] or with the Campbell/Switzer silver staining method for brain amyloid deposits [19]. The previously immunostained neurons were identified by vernier scale position and were found either to contain or to be devoid of argyrophilic material. This study does not intend to correlate the density of AT8-immunoreactive structures with the density of neurofibrillary changes as seen in silver-stained sections. The sensitivity of the Gallyas silver impregnation is not changed by the previous immunostaining and destaining of the chromogen.

Results

AT8-immunoreactive structures in the transentorhinal/entorhinal region

In general our cases which were devoid of neurofibrillary changes (stage 0; [11]) up to the age of 32 years, show at least rare immunoreactive neurites, while cases up to the age of 44 years exhibit some isolated group 1 pre-α neurons (see Table 1). In stage I cases a few to numerous group 1 to 3 pre-α neurons occur in both the transentorhinal and entorhinal region, single ones in the entorhinal layer pri-α. Cases of stages II-III exhibit numerous immunostained neurons within the transentorhinal region and the entorhinal layers pre-α and pri-α as well as some isolated neurons in the adjacent temporal isocortex. A dense network of neurites marks the descending transentorhinal layer pre-α and entorhinal layers pre-α/pre-β and pri-α.

Cases with rare or few immunostained neurons in the transentorhinal/entorhinal region permit correlation of immunoreactive cell bodies with immunostained cellular processes in their immediate surrounding. The majority of labeled nerve cells are unequivocally identifiable as pyramidal or modified pyramidal neurons. They do not show any spatial relationship to diffuse amyloid deposits. Dephosphorylation with alkaline phosphatase seems not to alter the staining properties for the AT8 antibody. It is important to note that several cases are free of silver-stained neurofibrillary changes (Table 1, stage 0), but display presence of AT8-immunoreactive nerve cells. Destaining the chromogene and restaining with the silver method permits direct comparison within the same section between the results of the two staining techniques. This procedure is used to classify the pathological changes of the immunoreactive neurons and to establish a morphological series possibly reflecting a sequence of changes undergone by the individual nerve cell as the disease process progresses. A similar series of alterations is also found in cortical pyramidal cells outside of the transentorhinal/entorhinal region. However, direct comparison between immunoreactivity and silver-staining capacity has only been carried out in the transentorhinal/entorhinal region. The distribution pattern of immunoreactive nerve cells closely corresponds to the pattern of neurofibrillary changes seen in the Gallyas-stained sections.

Group 1

Individual pyramidal neurons are completely labeled, including the dendritic arborisations and the axon, and thus resemble successfully stained neurons in Golgi impregnations (Figs. 1, 2, 10, 11). This immunostaining is considered to signify the first sign of cytoskeleton change. The reaction product appears granular or hatched and is loosely or densely distributed throughout the neuron (Figs. 12–14a, 23, 24). The thin axon is homogeneously stained, displays some dilations and can be traced for some distance (Figs. 10, 11). The axon staining apparently extends up into the terminals, because several elaborate axonal arborisations are encountered within the dendritic domain of group 1 neurons (Fig. 21a, b, c). Some coarse immunostained granules attched to the dendrites of immunostained neurons are considered to be afferent axonal terminals of unknown sources which also contain changed cytoskeleton material. At this time we cannot distinguish whether the alteration in the terminals is initiated by the cytoskeleton changes within the soma or whether the interaction occurs in the anterograde direction and these afferents represent a crucial input for the intact metabolism of the target neuron (Fig. 22a, b). The dendrites of several neurons even exhibit the presence of spines (Figs. 15, 16a, b).

The most conspicuous features of pyramidal cells in the transentorhinal layer pre-α are apical dendrites with terminal tufts (Figs. 1, 9). Distal parts of the apical dendrite and portions of the terminal tuft frequently exhibit intensely homogeneously stained rod-like inclusions, giving this part of the dendrite a slightly thickened appearance (Fig. 17a, b). In general, neurons with this quite normal appearance fail to reveal argyrophilic structures after the Gallyas silver impregnation (Figs. 32a, d, 32').

Group 2

Conspicuous changes in the neuronal processes occur that are not known to exist in pyramidal cells of the normal cerebral cortex. The terminal tuft and distal portions of the apical dendrite appear fragmented and/or completely lose their immunoreactivity. In place of the terminal tuft, numerous tortuous fibres with terminal swellings and blurred outlines are visible, as in growth cones (Figs. 18–20). The apical side branches and basal dendrites of the pyramidal neurons are still visible, but are conspicuously changed: their distal parts appear curved, exhibit thickened portions connected by thin segments, show appendages and/or T-shaped or multiple arborisation; the thickened portions contain homogeneously stained rod-like inclusions (Figs. 3–6, 25–27, 31a–d). The soma and proximal dendritic portions still contain granular and hatched material. Additionally, several rod-like inclusions are located in the soma, and preferentially in the branching points of the dendrites

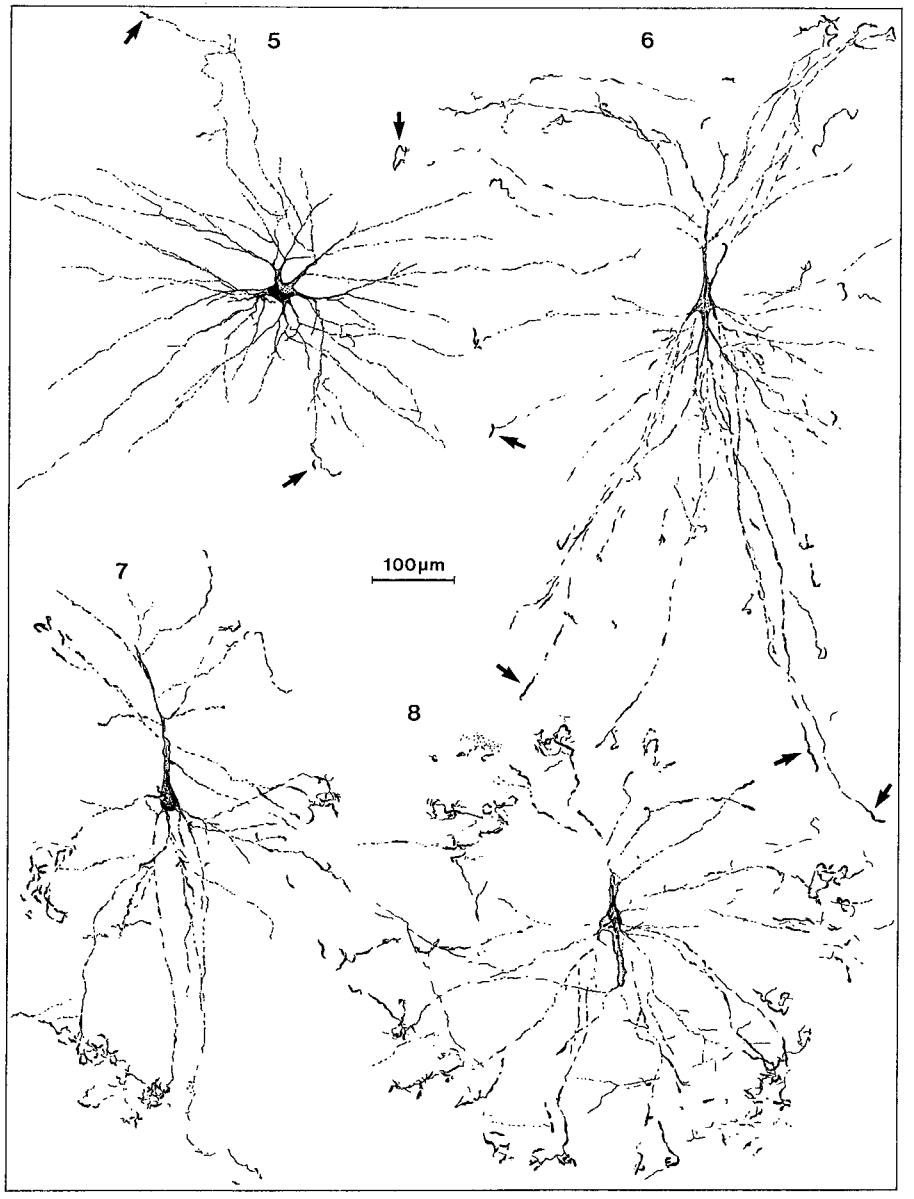

Figs. 1–8 Drawings from AT8-immunoreactive neurons. Cells **1** and **2**: pyramidal neurons from transentorhinal layer pre α. Cell **1** looks quite normal and belongs to the group 1 neurons. In cell **2** the terminal tuft of the apical dendrite appears fragmented, while the apical dendritic side branches and the basal dendrites look quite normal; cell **2** represents transition from group 1 to group 2 neurons. Cells **3–6**: modified pyramidal neurons from entorhinal layer pre α; they exhibit thickened and curved parts within their distal dendritic portions (*arrows*); these portions and the soma contain homogeneously stained rods. Rectangle (cell **3**) is shown at higher magnification in Figure 31c. Cell **7**, pyramidal neuron from CA1, and cell **8**, pyramidal neuron from subiculum, show heavily curved distal dendritic portions and fragmented middle portions of the dendrites; they are classified as group 3 neurons. Cell **1**: case 7, female 44 years; cells **2, 5, 6**: case 6, male 44 years; cells **3, 4**: case 10, male 51 years; cell **7**: case 11, female 55 years; cell **8**: case 17, male 66 years

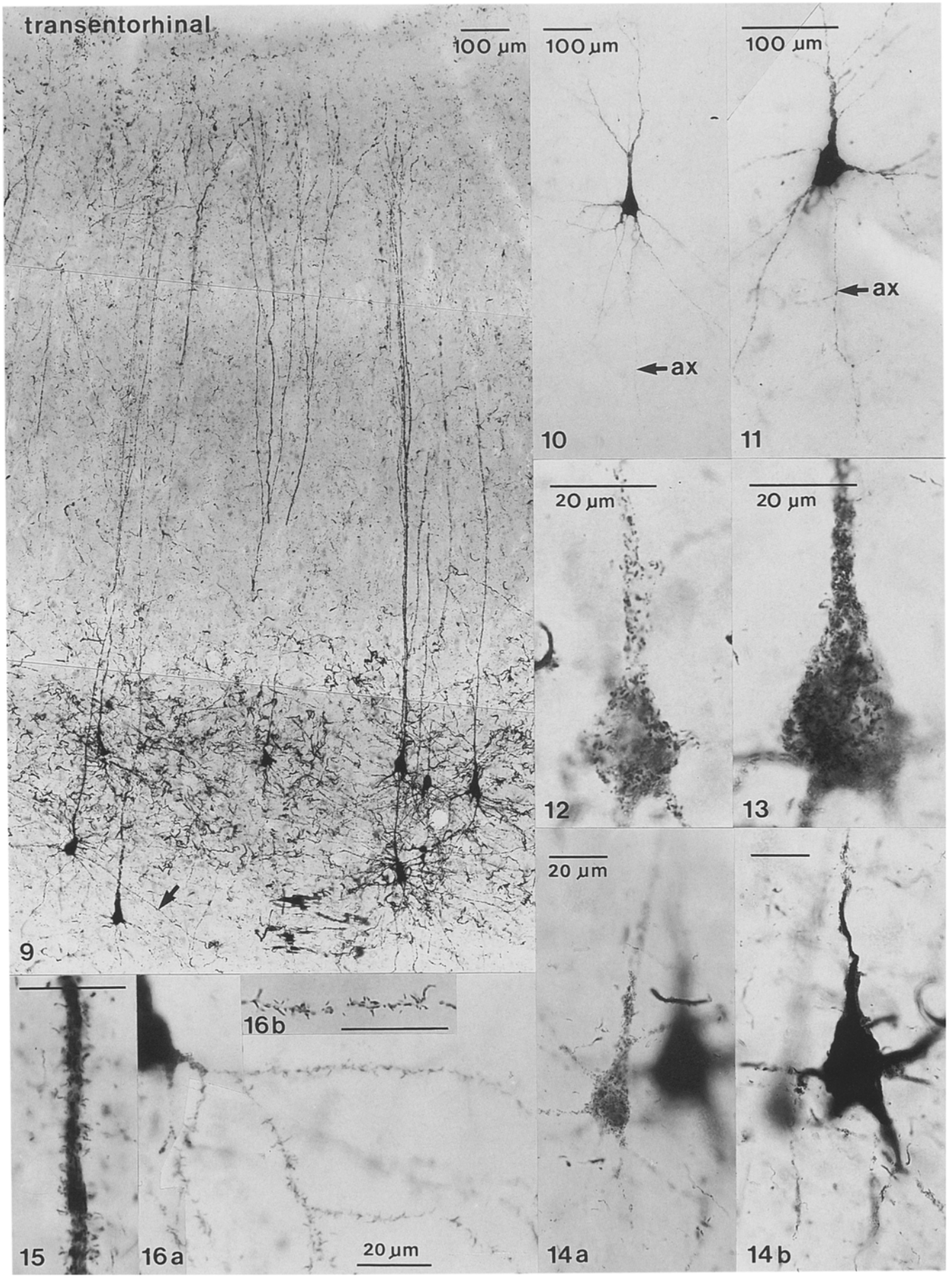

(for legends see page 560)

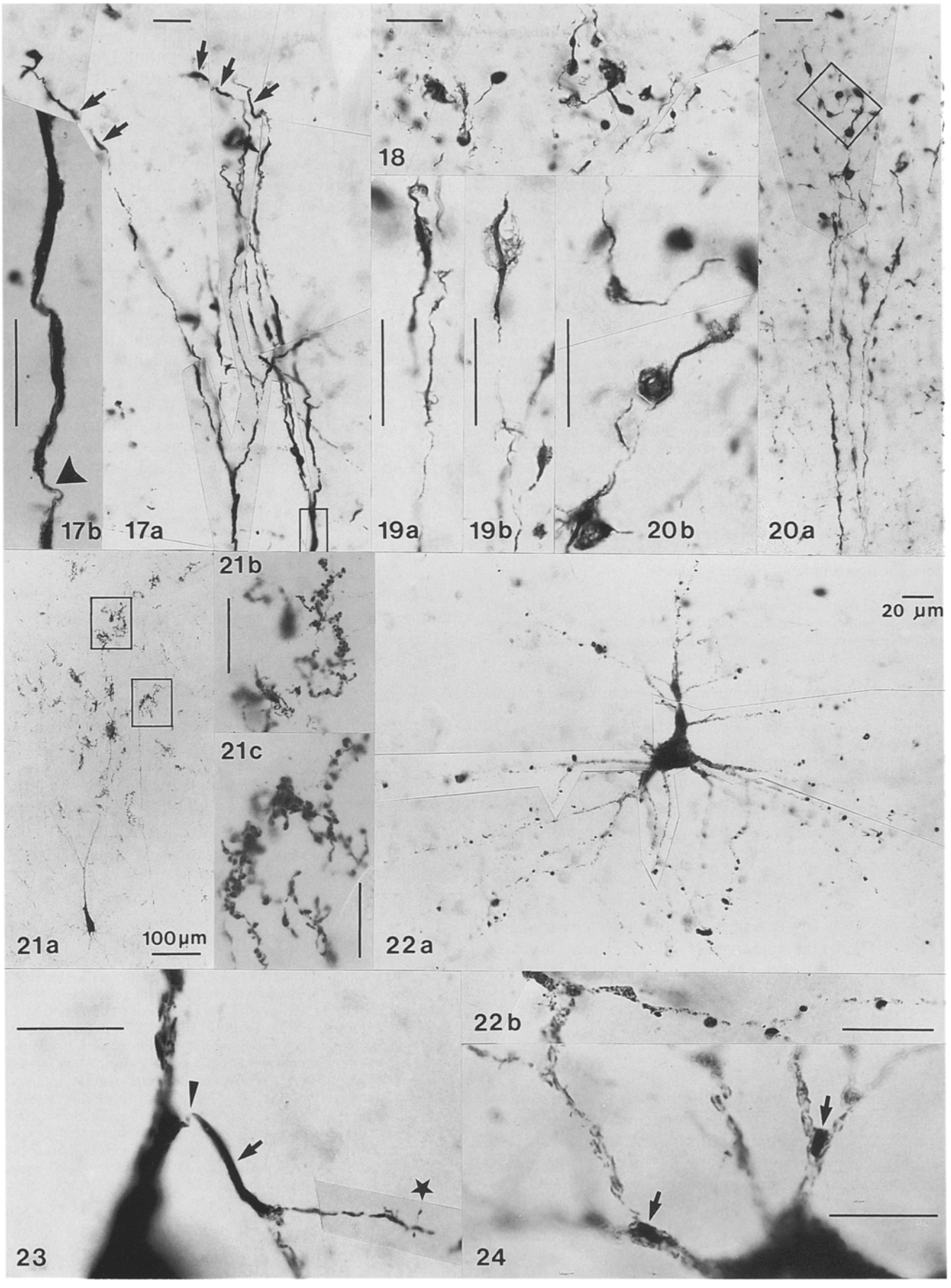

(for legends see page 560)

◀ **Figs. 9–16** Micrographs of AT8-immunoreactive structures. **9** Pyramidal neurons in the deep part of transentorhinal layer pre α are completely stained, including the apical dendrite with the terminal tuft and the basal dendrites (*arrow*). The curved fibres within the layer most likely represent previously affected basal dendrites. Pyramidal neurons, **10** from transentorhinal layer pre α, and **11** from entorhinal layer pre γ, show the dendritic tree and the axon (*ax*). Neurons **9–14a** exhibit a more or less densely granulated or hatched appearance. Neurons **9–14a** are classified as group 1 neurons. Cell **14a** is in close vicinity to an intensely homogeneously stained neuron **14b** (different levels of the focus), representing a group 3 neuron (transentorhinal layer pre α). **15** Apical dendrite of a pyramidal neuron (subiculum) and **16a,b** basal dendrites of a pyramidal neuron (entorhinal layer pre β) covered with spines. (**9**: case 16, female 64 years; **10, 11, 16**: case 6, male 44 years; **12–14**: case 15, male 64 years; **15**: case 26: female 77 years). *Bars* in **14b, 15**, and **16b** = 20 μm

◀ **Figs. 17–20** AT8-immunoreactive apical dendritic trees and terminal tufts of transentorhinal layer pre α pyramidal cells. **17a** Distal parts of the apical dendrite (*rectangle* at higher magnification in **17b**) and of the terminal tuft demonstrate thickened portions (*arrows*) which are connected by thin segments (*arrowhead*) (case 20: male 69 years). **18** Thickened tips of the terminal tuft probably associated with degenerating boutons. **19a, b** Distal tips of the terminal tuft showing thickened parts and parts with blurred outlines. **20** Terminal tuft with swellings, thickened and curved parts; *rectangle* is enlarged in the inset **20b** (**18–20**: case 15, male 64 years)

Fig. 21 AT8-immunostained pyramidal neuron (**a**) of sector CA1 with axonal arborizations (enlarged in the *insets* **b, c**) within the dendritic domain (case 12: male 57 years)

Fig. 22 AT8-immunostained pyramidal cell of entorhinal layer pre γ (**a**) showing numerous globules attached to the dendrites, probably representing degenerating boutons, pictured at higher magnification in the *inset* **22b** (case 10: male 51 years)

Fig. 23 AT8-immunoreactive pyramid-like neuron of the lateral amygdaloid nucleus, corresponding to group 2 neurons. A thickened part (*arrow*) in a dendritic side branch is connected by a thin segment (*arrowhead*) to the dendritic stem and continues with a quite normal appearance with dendritic spines (*asterisks*) (case 6: male 44 years)

Fig. 24 Part of the AT8-immunoreactive neuron 8 demonstrating immunoreactive rods in the dendritic branching points (*arrows*) (case 6: male 44 years). *Bars* in **17–20**, **21b–24** = 20 μm

(Figs. 23, 24). In general, the axon is no longer visible (Figs. 3–7). In most neurons, Gallyas staining reveals a small NFT in the soma (Fig. 32e,e') and NT in several curved distal parts of the dendrites.

Group 3

At this level of destruction the perikarya of pyramidal neurons and their proximal dendritic stumps are intensely and homogeneously immunostained (Figs. 14b, 28–30). The intermediate parts of the dendrites appear fragmented or lose immunoreactivity. The distal dendritic parts consist of multiple thickened segments containing rod-like inclusions; they appear heavily curved and branched and are generally separated from the parent soma; thus, they surround the soma like a corona (diameter about 600–900 μm; Figs. 7, 8, 28–30). The alterations in the distal parts of the basal dendrites appear more pronounced than those in the apical side branches. Gallyas staining of the same neuron reveals a classic NFT within the soma (Fig. 32b,b', c,c') and neuropil threads in numerous curved distal parts of the dendrites.

Group 4

The location of the perikaryon is roughly marked by an accumulation of coarse immunostained granules of various sizes and by fine fibres. Gallyas staining reveals a NFT; occasionally the fibrillary material is less tightly packed (Fig. 32f,f', g,g'); a nucleus is no longer visible. This group probably represents the transition from an intracellular to an extracellular NFT ("early" ghost tangle).

Group 5

AT8-immunoreactive structures are not visible, but staining with Gallyas silver impregnation reveals a NFT in the section, which corresponds to a "tombstone" or ("late") ghost tangle (Fig. 32h').

AT8-immunoreactive structures in other areas of the section

Depending on the stage of neurofibrillary changes in areas adjacent to the entorhinal region, somata and processes may be immunostained. Neurons unequivocally identified as pyramidal neurons show alterations similar to those described. Differently formed neurons may also be stained. It is not unusual to find immunostained neurons in the amygdaloid nuclei.

Alz-50-immunoreactive structures

In sections immunostained with Alz-50 adjacent to those stained with AT8, distinctly fewer somata and fibres are visible. In principle, classification of entorhinal and transentorhinal pyramidal neurons into groups similar to those in the AT8 staining can be done, but the appearance, sequence and differences are less distinct. Neurons surrounded by a "corona" of more or less heavily curved distal dendritic parts are also present, similar to those shown by Sparks et al. ([54], his Fig. 4) (corresponding to AT8 group 2 and 3); Gallyas silver impregnation reveals a classic NFT in the soma (Fig. 34,34' arrow). Neurons resembling the "tangle-associated neuritic clusters", TANC, of Munoz et al. [47] probably represent "early" ghost tangles (Fig. 33,33'), while "late" ghost tangles (Fig. 34,34') correspond to AT8 group 5 structures.

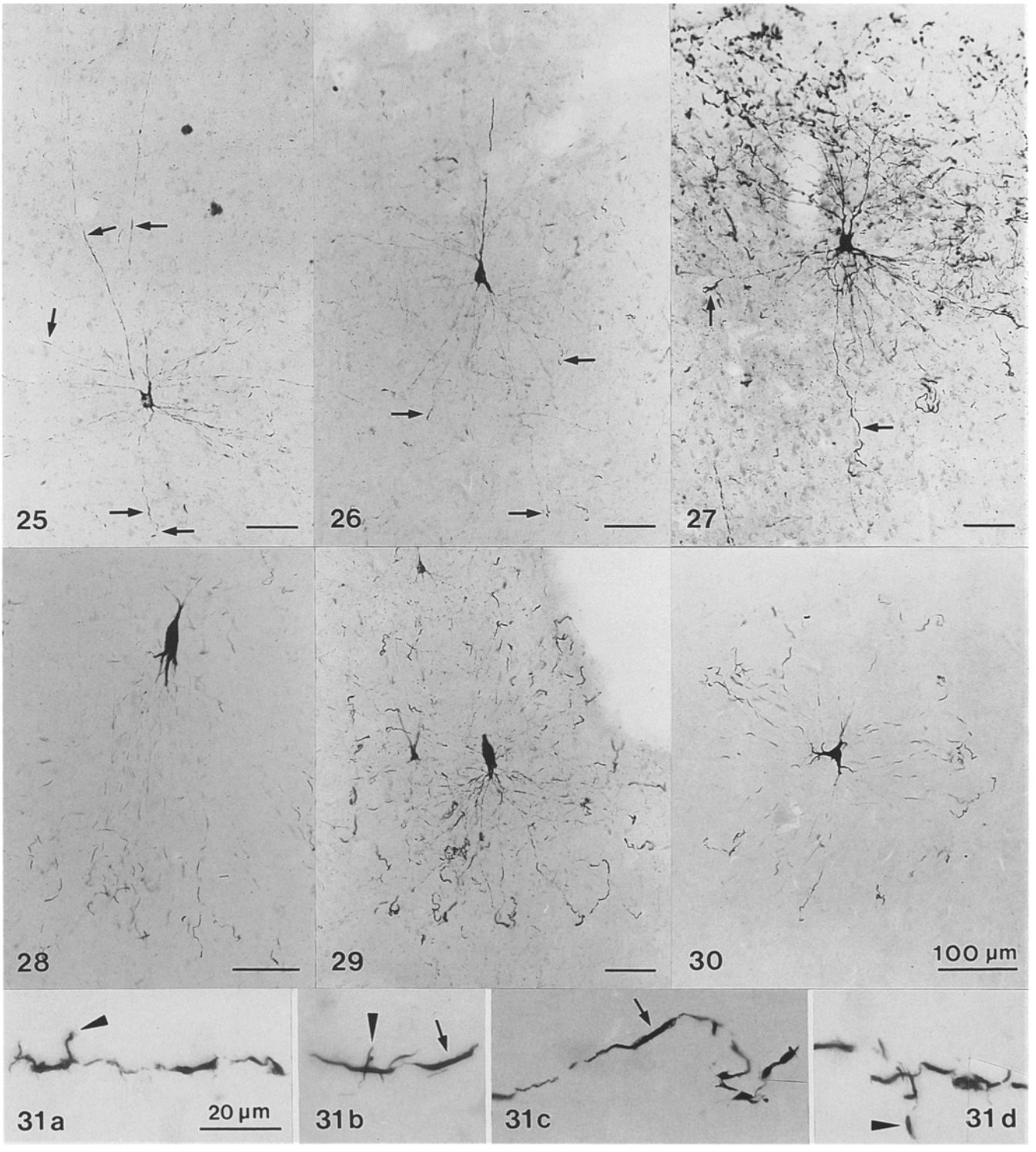

Figs. 25–27 AT8-immunoreactive group 2 neurons: most dendrites are visible and show thickened parts and curved distal parts [*arrows*: **25**: entorhinal layer pre γ (case 10), **26**: transentorhinal layer pre β (case 12), **27**: entorhinal layer pre α (case 16)]. *Bars* in **25–27** = 100 µm

Figs. 28–30 AT8-immunoreactive group 3 neurons: most dendrites are no longer visible; note the curved dendritic tips surrounding the soma like a corona (**28**: entorhinal layer pre α (case 12), **29**: transentorhinal layer pre α (case 12), **30**: entorhinal layer pre γ (case 5)). *Bars* in **28–30** = 100 µm

Fig. 31a–d Curved and thickened distal dendritic parts with rod-like inclusions (*arrows*) and appendages or outgrowths (*arrowheads*) from AT8-immunoreactive neurons group 2 and 3. **c** shows the rectangle of neuron 4 at higher magnification (case 6). *Bar* is also valid for **b–d**

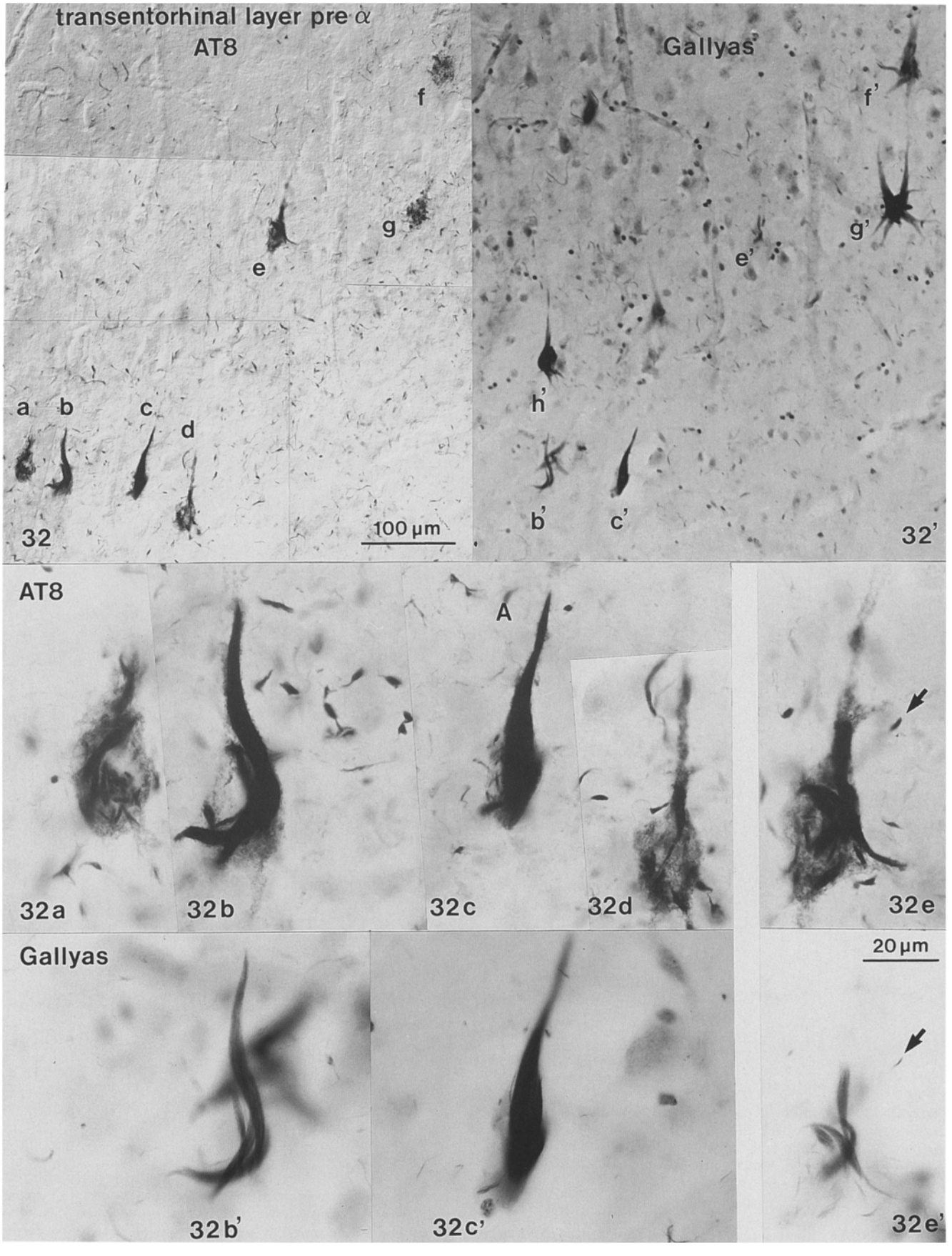
transentorhinal layer pre α
AT8
Gallyas
a
b
c
d
e
f
g
h'
b'
c'
e'
f'
g'
32
32'
100 µm
AT8
A
32a
32b
32c
32d
32e
Gallyas
20 µm
32b'
32c'
32e'

◀ **Fig. 32** Low-power view of the descending transentorhinal layer pre α immunostained with AT8, and **32'** after de-staining the chromogen and re-staining with the Gallyas silver impregnation for neurofibrillary changes. The AT8-stained neurons are shown a higher magnification in the *second row* of this and the *first row* on the next figure panel, while the same neurons after Gallyas staining are shown in the *third row* of this and the *second row* of the next figure panel. Neurons **a** and **d** contain immunoreactive granular material and small rods. They are not stained with Gallyas method (group 1 neurons, see empty space beside **b'** and **c'**). Neurons **b** and **c** exhibit densely immunostained fiber bundles which appear as "classic" neurofibrillary tangles in the Gallyas staining (**b'** and **c'**; group 3 neurons). The immunostained neuron **e** harbours several rod-like inclusions and shows in Gallyas staining a small neurofibrillary tangle (NFT: **e'**; group 2 neuron). Structures **f** and **g** are marked by numerous degenerating immunostained terminals attached to the somata, the contours of which are no longer visible. In Gallyas impregnation densely stained fiber bundles appear (**f'** and **g'**) representing the transition from an intracellular to an extracellular NFT ("early" ghost tangle, group 4 structures). Structure **h'** is not immunostained but is present in the Gallyas impregnation and is considered to represent a "late" ghost tangle (group 5 structure). *Arrows* point to identical structures in the neuropil (case 29, male 81 years)

Figs. 33–34 Alz-50-immunostained structures in the entorhinal layer pre α, **33'** and **34'** after de-staining and re-staining with the Gallyas impregnation. Structure **33** is marked by numerous attached degenerating terminals and is considered to be an "early" ghost tangle. *Arrows* point to identical structures in the neurophil. **34** shows an intensely immunostained neuron (*arrow*) which in **34'** turns out to be a classic NFT among three "late" ghost tangles (not visible in **34**; case 29). *Bar* in **34** is also valid for **33**
▼

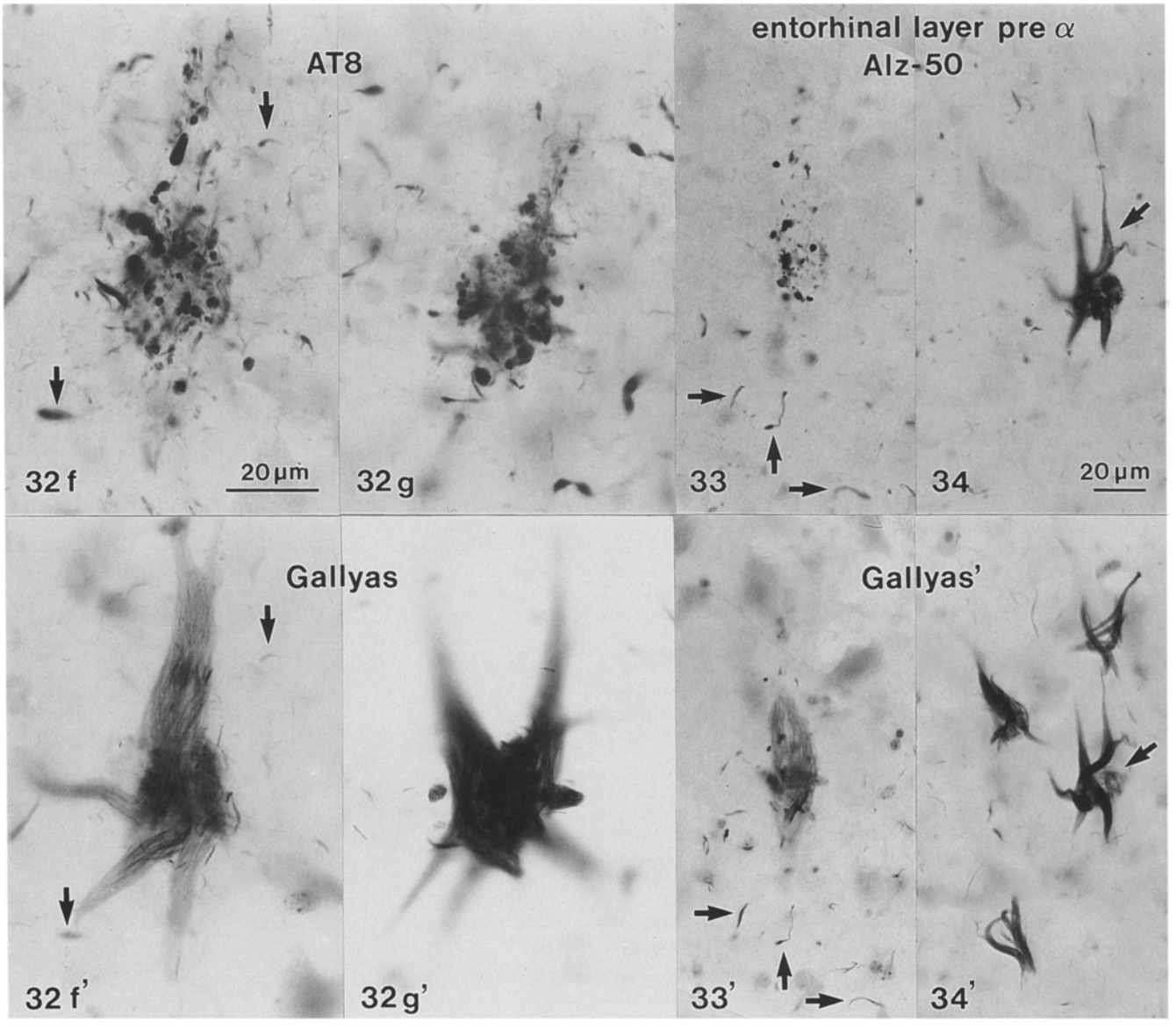

Discussion

Hypothesized development of cytoskeletal alterations

Alzheimer [1] and Bielschowsky [3] already distinguished between intracellular and extraneuronal NFT. However, very early events in the development of neurofibrillary changes can only be appropriately studied by immunocytochemical methods because, obviously, the biochemical changes antecede the morphological alteration. Bancher et al. [2] defined three different maturation stages of NFT using immunocytochemical reactivities with mono- and polyclonal antibodies to tau and ubiquitin. At their stage 0 a number of morphologically normal pyramidal cells show diffuse or fine granular cytoplasmic staining with anti-tau; at stage 1 some delicate elongate inclusions are stained by tau antibodies and in silver impregnations (early tangles); stage 2 is represented by the classic NFT demonstrated both with anti-tau and in silver impregnations; stage 3 is examplified by ghost tangles, which are characterised by a reduced anti-tau but marked anti-ubiquitin immunostaining. The density of stage 0 and 1 neurons stained with anti-tau is higher than the number of tangles in the adjacent silver-stained sections. As in our results, this proposed sequence provides evidence that the appearance of abnormally phosphorylated tau precedes the formation of NFT stained by silver impregnation methods ([24, 36, 40, 45, 57]; see Table 2).

Group 1

Our group 1 neurons probably correspond to stage 0 neurons of Bancher et al. [2]. In our opinion, the granular staining of the cytoplasm with AT8 represents the earliest degenerative change of the cytoskeleton (Fig. 35). The neurons are stained with sufficient detail to assess the dendritic pattern, the presence of dendritic spines, and the axon, but all parts of the neuron already contain the abnormally phosphorylated tau protein. The majority of our cases are devoid of amyloid deposits and neuritic plaques (Table 1). This provides some evidence that in the transentorhinal/entorhinal region this alteration occurs as the result of an intrinsic process rather than the alterations are induced by environmental factors such as the presence of diffuse plaques (amyloid deposits) or neuritic plaques [28, 50].

Probably, it remains a possibility that the AT8-positive group 1 cells may reverse the cytoskeleton changes and recover, namely when their distal dendritic portions have not yet changed. After the development of the curved distal dendritic parts with rod-like inclusions, the destructive process will almost certainly continue its downhill course.

Group 2

Group 2 cells display conspicuous changes of the terminal tuft of the apical dendrite. Therefore, afferents from

Table 2 Proposed sequence of cytoskeletal changes in cortical pyramidal cells leading to neurofibrillary tangles in AD (*AD* Alzheimer's disease, *i-cellular* intracellular, *e-cellular* extracellular, *ir* immunoreactive, *ir-rods* intensely homogeneously immunostained rod-like inclusions, *m-anti-tau* monoclonal antibody, *NFT* neurofibrillary tangles, *p-anti-tau* polyclonal antibody, *PHF* paired helical filaments)

	Granular hatched material	Fibrillar inclusions	Compact fiber bundles classic tangle	Transition i-cellular/ e-cellular tangle	Extra-cellular tangle
Bancher et al. [2] m-anti-tau/ p-anti-tau	**Stage 0** Selective staining of normal pyramidal cells	**Stage 1** Some delicate elongate inclusions	**Stage 2** Classic NFT		**Stage 3** Ghost tangle
Duong et al. [24] anti-tau	**Stage 0** Granular labeling in soma	**Stage 1** Fibrillar structures in soma and proximal processes of primary dendrites	**Stage 2** NFT displace cytoplasm and nucleus		**Stage 3** NFT with no visible soma or nucleus
Braak et al. [16] anti-PHF-tau-AT8	**Group 1** Granular hatched material in soma, dendrites, axon, "normal" Golgi-like appearance of pyramidal neurons	**Group 2** Apical terminal tuft lost, apical dendrite truncated, ir-rods in soma and dendrites, curved distal dendritic parts, axon no longer visible	**Group 3** Intense staining of the soma, heavy curving in distal dendritic parts intermediate dendritic part not visible	**Group 4** Coarse ir-granules mark position of the soma	**Group 5** No staining
Silver stain (Gallyas)	No staining	Singular fibre bundles	Classic NFT	"Early" ghost tangles	"Late" ghost tangles

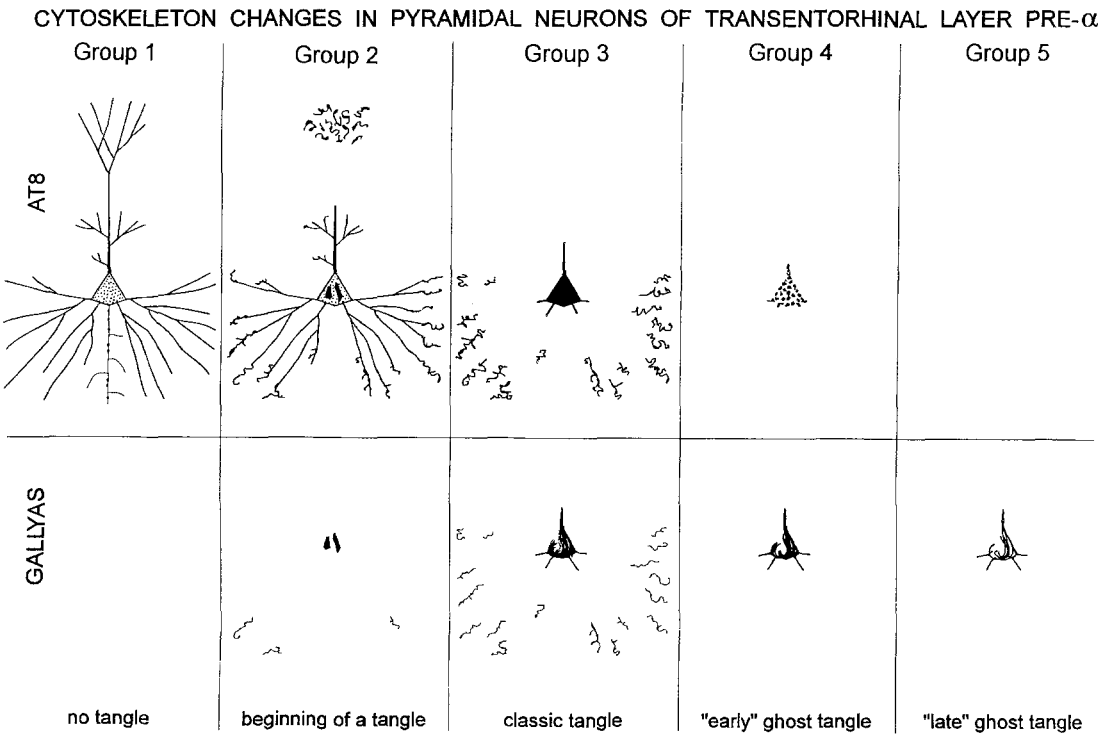

Fig. 35 Schematic drawing summarizing AT8 immunostaining with the corresponding Gallyas silver staining. The progression of pathological alterations of the neuronal cytoskeleton is shown from group 1 neuron to group 5 structure. *Fine dots* indicate granular AT8 immunostaining, while *large dots* represent degenerating terminals attached to the disintegrated cell body

axons running within the molecular layer may be among the first connections to be destroyed.

Microfilaments, intermediate filaments, microtubules, and their associated proteins assemble to form the cytoskeleton. One of its functions is to control the shape of the soma and its processes [18, 41]. A dense network of microfilaments beneath the plasma membrane, consisting essentially of actin, provides the cell surface with mechanical strength. Tau and other microtubule-associated proteins stabilize and bundle microtubules and play an important role in the formation of cellular processes [25]. Abnormal phosphorylation sites on tau proteins probably destabilize microtubules [5] and may lead to conditions similar to axonal growth cones. The blurred outlines of the distal tips of the apical terminal tuft, as well as the multiple outgrowths and curving in the distal dendritic tips, bear some resemblance with axonal growth cones. However, only in rare cases do the curved distal dendritic parts show GAP 43 immunoreactivity ([53] neuron-specific phosphoprotein B-50 is implicated in neurite outgrowth). This might be because they are of dendritic origin and/or because they are pathologically changed.

In vitro, all tau isoforms have a tendency to self-assemble and polymerize into fibres [59]. Similar events might take place in vivo. The homogeneously stained rod-like inclusions might represent an irreversible alteration within the cell, consisting of pathological cytoskeleton elements, which can also be visualised after silver staining. They are considered to represent alterations in the process of formation of the argyrophilic NFT (group 2 and 3 neurons) and NT. The NT possibly "grow" at both ends [39]. However, NT are very rarely seen in continuity with the parent soma [37, 52].

Group 3

Group 3 neurons with heavily curved distal dendritic tips correspond to stage 2 neurons of Bancher et al. [2].

Group 4

The group 4 structures represent the degradation of the cellular entity. The cell membrane eventually disintegrates and the intracellular NFT becomes an extracellular one. During this transition the amino terminus and part of the carboxy terminus of the tau molecule is lost [7, 23, 26]; thus the staining properties change. Synaptic boutons and neurites formerly attached to the cell membrane may undergo degeneration and be immunostained; they roughly mark the position of the neuron. Group 4 structures correspond to the NFT described by others [38, 47, 58, 63]. It is not uncommon for afferents to remain attached to atrophying dendrites for a while [22].

Group 5

NFT shown with silver-impregnations techniques that are not associated with either Nissl substance and nucleus or with AT8 or with Alz-50 immunoreactivity are considered to be extracellular tangles (ghost or tombstone tangles). They correspond to stage 3 tangles of Bancher et al. [2].

In conclusion, this study shows the presence of abnormally phosphorylated tau protein in the entire nerve cell prior to the development of argyrophilic neurofibrillary changes. Particularly conspicuous are changes of the distal dendritic parts which precede the formation of NT. Such alterations are only seen in cortical neurons susceptible to the development of neurofibrillary changes. Cells of this type in the transentorhinal and entorhinal regions are among the first neurons in the entire brain to develop the cytoskeleton changes. The fact that this generally occurs in the absence of amyloid deposits favours the opinion that the pathological process is initiated by intrinsic events rather than by influences from the surrounding tissue. Probably, there exists the possibility that group 1 neurons (without destruction of their neuronal processes) reverse the early cytoskeleton changes and recover, an aspect which provides a possibility to develop new therapeutic strategies.

Acknowledgements The skillful technical assistance of Mrs. A. Biczysko and U. Rose is gratefully acknowledged. The authors thank Profs. K. Hübner and J. Stutte, Senckenbergisches Pathologisches Institut of the J.W. Goethe-University, Frankfurt and Prof. H.H. Goebel and Dr. J. Bohl, Institute for Neuropathology, J. Gutenberg University, Mainz, for providing the autopsy material. We thank Prof. P. Davies for his generous gift of the Alz-50 antibody and Dr. A. Van de Voorde, Innogenetics Gent, Belgium, for the antibody AT8. We thank Mrs. I. Szasz for the drawings and Mrs. U. Trautmann for photographic aid.

References

1. Alzheimer A (1911) Über eigenartige Krankheitsfälle des späteren Alters. Z Gesamte Neurol Psychiatr 4: 356–385
2. Bancher C, Brunner C, Lassmann H, Budka H, Jellinger K, Wiche G, Seitelberger F, Grundke-Iqbal I, Wisniewski HM (1989) Accumulation of abnormally phosphorylated τ precedes the formation of neurofibrillary tangles in Alzheimer's disease. Brain Res 477: 90–99
3. Bielschowsky M (1911) Zur Kenntnis der Alzheimer'schen Krankheit (präsenilen Demenz mit Herdsymptomen). J Psychol Neurol 18: 273–292
4. Biernat J, Mandelkow E-M, Schröter E, Lichtenberg-Kraag B, Steiner B, Berling B, Meyer H, Mercken M, Vandermeeren A, Goedert M, Mandelkow E (1992) The switch of tau protein to an Alzheimer-like state includes the phosphorylation of two serine-proline motifs upstream of the microtubule binding region. EMBO J 11: 1593–1597
5. Biernat J, Gustke N, Drewes G, Mandelkow E-M, Mandelkow E (1993) Phosphorylation of serine 262 strongly reduces the binding of tau protein to microtubules: distinction between PHF-like immunoreactivity and microtubule binding. Neuron 11: 153–163
6. Bondareff W, Wischik CM, Novak M, Amos WB, Klug A, Roth M (1990) Molecular analysis of neurofibrillary degeneration in Alzheimer's disease. An immunohistochemical study. Am J Pathol 137: 711–723
7. Bondareff W, Wischik CM, Novak M, Roth M (1991) Sequestration of tau by granulovacuolar degeneration in Alzheimer's disease. Am J Pathol 139: 641–647
8. Braak E, Strotkamp B, Braak H (1991) Parvalbumin immunoreactive structures in the hippocampus of the human adult. Cell Tissue Res 264: 33–48
9. Braak H, Braak E (1985) On areas of transition between entorhinal allocortex and temporal isocortex in the human brain. Normal morphology and lamina-specific pathology in Alzheimer's disease. Acta Neuropathol (Berl) 68: 325–332
10. Braak H, Braak E (1989) Cortical and subcortical argyrophilic grains characterize a disease associated with adult onset dementia. Neuropathol Appl Neurobiol 15: 13–26
11. Braak H, Braak E (1991) Neuropathological stageing of Alzheimer-related changes. Acta Neuropathol 82: 239–259
12. Braak H, Braak E (1992) The human entorhinal region. Normal morphology and lamina-specific pathology in various diseases. Neurosci Res 15: 6–31
13. Braak H, Braak E, Strenge H (1976) Gehören die Inselneurone der Regio entorhinalis zur Klasse der Pyramiden- oder der Sternzellen? Z Mikrosk Anat Forsch 90: 1017–1031
14. Braak H, Braak E, Grundke-Iqbal I, Iqbal K (1986) Occurrence of neuropil threads in the senile human brain and in Alzheimer's disease: a third location of paired helical filaments outside of neurofibrillary tangles and neuritic plaques. Neurosci Lett 65: 351–355
15. Braak H, Braak E, Ohm T, Bohl J (1988) Silver impregnation of Alzheimer's neurofibrillary changes counterstained for basophilic material and lipofuscin pigment. Stain Technol 63: 197–200
16. Braak H, Duyckaerts C, Braak E, Piette F (1993) Neuropathological staging of Alzheimer-related changes correlates with psychometrically assessed intellectual status. In: Corian B, Iqbal K, Nicolini M, Winblad B, Wisniewski H, Zatta P (eds) Alzheimer's disease: advances in clinical and basic research. Third International Conference on Alzheimer's Disease and Related Disorders. John Wiley & Sons, Chichester, pp 131–137
17. Bramblett GT, Trojanowski JQ, Lee VM-E (1992) Regions with abundant neurofibrillary pathology in human brain exhibit a selective reduction in levels of binding-competent τ and accumulation of abnormal τ-isoforms (A68) proteins. Lab Invest 66: 212–222
18. Cacares A, Kosik KS (1990) Inhibition of neurite polarity by tau antisense oligonucleotides in primary cerebellar neurons. Nature 343: 461–463
19. Campbell SK, Switzer RC, Martin TL (1987) Alzheimer's plaques and tangles: a controlled and enhanced silver-staining method. Soc Neurosci Abstr 13: 678
20. Caputo CB, Wischik C, Novak M, Soctt CW, Brunner WF, Montejo de Garcini E, Lo MMS, Norris TE, Salama AI (1992) Immunological characterization of the region of tau protein that is bound to Alzheimer paired helical filaments. Neurobiol Aging 13: 267–274
21. Delacourte A, Defossez A (1986) Alzheimer's disease: tau proteins, the promoting factors of microtubule assembly, are major components of paired helical filaments. J Neurol Sci 76: 173–186
22. Deitch JS, Rubel EW (1989) Rapid changes in ultrastructure during deafferentiation-induced dendritic atrophy. J Comp Neurol 281: 234–258
23. Dickson DW, Ksiezak-Reding H, Liu W-K, Davies P, Crowe A, Yen S-HC (1992) Immunocytochemistry of neurofibrillary tangles with antibodies to subregions of tau protein: identification of hidden and cleaved tau epitopes and a new phosphorylation site. Acta Neuropathol 84: 596–605
24. Duong T, Doucette T, Zidenberg NA, Jacobs RW, Scheibel AB (1993) Microtubule-associated proteins tau and amyloid P component in Alzheimer's disease. Brain Res 603: 74–86
25. Edson K, Weisshaar B, Matus A (1993) Actin depolymerisation induces process formation on MAP2-transfected non-neuronal cells. Development 117: 689–700

26. Endoh R, Ogawara M, Iwatsubo T, Nakano I, Mori H (1993) Lack of the carboxyl-terminal sequence of tau in ghost tangles of Alzheimer's disease. Brain Res 601: 164–172
27. Feldman M (1984) Morphology of the neocortical pyramidal neuron. In: Peters A, Jones EG (eds) Cerebral cortex. Cellular components of the cerebral cortex, vol 1. Plenum Press, New York, pp 123–200
28. Ferrer I, Guionnet N, Cruz-Sánchez F, Tuñón T (1990) Neuronal alterations in patients with dementia: a Golgi study on biopsy samples. Neurosci Lett 114: 11–16
29. Gallyas F (1971) Silver staining of Alzheimer's neurofibrillary changes by means of physical development. Acta Morphol Acad Sci Hung 19: 1–8
30. Goedert M, Wischik CM, Crowther RA, Walker JE, Klug A (1988) Cloning and sequencing of the cDNA encoding a core protein of the paired helical filament of Alzheimer's disease: identification as the microtubule-associated protein tau. Proc Natl Acad Sci USA 85: 4051–4055
31. Goedert M, Spillantini MG, Jakes R (1991) Localization of the Alz-50 epitope in recombinant human microtubule-associated tau. Neurosci Lett 126: 149–154
32. Goedert M, Jakes R, Crowther RA, Six J, Vandermeeren M, Cras P, Trojanowski JQ, Lee VM-Y (1993) The abnormal phosphorylation of tau protein at Ser-202 in Alzheimer disease recapitulates phosphorylation during development. Proc Natl Acad Sci USA 90: 5066–5070
32. Greenberg SG, Davies P (1990) A preparation of Alzheimer paired helical filaments that displays distinct τ proteins by polyacrylamide gel electrophoresis. Proc Natl Acad Sci USA 87: 5827–5831
34. Grundke-Iqbal I, Iqbal K, Tung Y-C, Quinlan M, Wisniewski HM, Binder LI (1986) Abnormal phosphorylation of the microtubule-associated protein τ (tau) in Alzheimer cytoskeletal pathology. Proc Natl Acad Sci USA 83: 4913–4917
35. Grundke-Iqbal I, Vorbrodt A, Iqbal K, Tung Y-C, Wang GP, Wisniewski HM (1988) Microtubule-associated polypeptides tau are altered in Alzheimer paired helical filaments. Mol Brain Res 4: 43–52
36. Hyman BT, van Hoesen GW, Wolozin BL, Davies P, Kromer LJ, Damasio AR (1988) Alz-50 antibody recognizes Alzheimer-related neuronal changes. Ann Neurol 23: 371–379
37. Ihara Y (1988) Massive somatodendritic sprouting of cortical neurons in Alzheimer's disease. Brain Res 459: 138–144
38. Ikeda K, Haga C, Oyanagi S, Iritani S, Kosaka K (1992) Ultrastructural and immunohistochemical study of degenerate neurite-bearing ghost tangles. J Neurol 239: 191–194
39. Iwatsubo T, Hasegawa M, Esaki Y, Ihara Y (1992) Lack of ubiquitin immunoreactivities at both ends of neuropil threads. Possible bidirectional growth of neuropil threads. Am J Pathol 140: 277–282
40. Joachim CL, Morris JH, Selkoe DJ, Kosik KS (1987) Tau epitopes are incorporated into a range of lesions in Alzheimer's disease. J Neuropathol Exp Neurol 46: 611–622
41. Kirkeeide E-K, Pryme IF, Vedeler A (1993) Microfilaments and protein synthesis; effects of insulin. Int J Biochem 25: 853–864
42. Kondo J, Honda T, Mori H, Hamada Y, Miura R, Ogawara M, Ihara Y (1988) The carboxyl third of tau is tightly bound to paired belical filaments. Neuron 1: 827–834
43. Kosik KS, Joachim CL, Selkoe DJ (1986) Microtubule-associated protein tau (τ) is a major antigenic component of paired helical filaments in Alzheimer's disease. Proc Natl Acad Sci USA 83: 4044–4048
44. Ksiezak-Reding H, Chien CH, Lee VMY, Yen SH (1990) Mapping of the Alz-50 epitope in microtubule-associated protein tau. J Neurosci Res 25: 412–419
45. Masliah E, Iimoto DS, Mallory M, Albright T, Hansen L, Saitoh T (1992) Casein kinase II alteration tau accumulation in tangle formation. Am J Pathol 140: 263–268
46. Mercken M, Vandermeeren M, Lübke U, Six J, Boons J, Van de Voorde A, Martin J-J, Gheuens J (1992) Monoclonal antibodies with selective specifity for Alzheimer tau are directed against phosphatase-sensitive epitopes. Acta Neuropathol 84: 265–272
47. Munoz DG, Wang D (1992) Tangle-associated neuritic clusters. A new lesion in Alzheimer's disease and aging suggests that aggregates of dystrophic neurites are not necessarily associated with β/A4. Am J Pathol 140: 1167–1178
48. Novak M, Kabat J, Wischik CM (1993) Molecular characterization of the minimal protease resistant tau-unit of the Alzheimer's disease paired helical filament. EMBO J 12: 365–370
49. Nukina N, Kosik KS, Selkoe DJ (1988) The monoclonal antibody, Alz 50, recognizes tau proteins in Alzheimer's disease brain. Neurosci Lett 87: 240–246
50. Probst A, Basler V, Brion B, Ulrich J (1983) Neuritic plaques in senile dementia of Alzheimer type: a Golgi analysis in the hippocampal region. Brain Res 268: 249–254
51. Rye DB, Leverenz J, Greenberg SG, Davies P, Saper CB (1993) The distribution of Alz-50 immunoreactivity in the normal human brain. Neuroscience 56: 109–127
52. Schmidt ML, Murray JM, Trojanowski JQ (1993) Continuity of neuropil threads with tangle-bearing and tangle-free neurons in Alzheimer disease cortex. A confocal laser scanning microscopy study. Mol Chem Neuropathol 18: 299–312
53. Six J, Lübke U, Lenders MB, Vandermeeren M, Mercken M, Villanova M, van de Voorde A, Gheuens J, Martin J-J, Cras P (1992) Neurite sprouting and cytoskeletal pathology in Alzheimer's disease: a comparative study with monoclonal antibodies to growth-associated protein B-50 (GAP43) and paired helical filaments. Neurodegeneration 1: 247–255
54. Sparks DL, Huaichen L, Scheff SW, Coyne CM, Hunsaker JC III (1993) Temporal sequence of plaque formation in the cerebral cortex of non-demented individuals. J Neuropathol Exp Neurol 52: 135–142
55. Szendrei GI, Lee VM-Y, Otvos L (1993) Recognition of the minimal epitope of monoclonal antibody tau-1 depends upon the presence of a phosphate group but not its location. J Neurosci Res 34: 243–249
56. Ueda K, Masliah E, Saitoh T, Bakalis SL, Scoble H, Kosik KS (1990) Alz-50 recognizes a phosphorylated epitope of tau protein. J Neurosci 10: 3295–3304
57. Ulrich J, Anderton BH, Brion J-P, Euler M, Probst A (1987) Cytoskeletal immunohistochemistry of Alzheimer's disease. J Neural Transm [Suppl] 24: 197–204
58. Vande Weghe J, Cras P, Kawai M, Siedlak SL, Tabaton M, Greenberg B, Perry G (1991) Dystrophic neurites infiltrate extracellular neurofibrillary tangles in Alzheimer disease. Brain Res 560: 303–305
59. Wille H, Drewes G, Biernat J, Mandelkow E-M, Mandelkow E (1992) Alzheimer-like paired helical filaments and antiparallel dimers formed from microtubule-associated protein tau in vitro. J Cell Biol 118: 573–584
60. Wischik CM, Novak M, Thogersen H, Edwards P, Runswick M, Jakes R, Walker J, Milstein C, Roth M, Klug A (1988) Isolation of a fragment of tau derived from the core of the paired helical filament of Alzheimer disease. Proc Natl Acad Sci USA 85: 4506–4510
61. Wolozin BL, Pruchnicki A, Dickson DW, Davies P (1986) A neuronal antigen in the brains of Alzheimer patients. Science 232: 648–650
62. Wood JG, Mirra SS, Pollock NJ, Binder LI (1986) Neurofibrillary tangles of Alzheimer disease share antigenic determinants with the axonal microtubule-associated protein tau (τ). Proc Natl Acad Sci USA 83: 4040–4043
63. Yamaguchi H, Nakazato Y, Kawarabayashi T, Ishiguro K, Ihara Y, Morimatsu M, Hirai S (1991) Extracellular neurofibrillary tangles associated with degenerating neurites and neuropil threads in Alzheimer-type dementia. Acta Neuropathol 81: 603–609